

# Insights on Immobilization of Cd Contamination in Soil: Synergic Impacts of Water Management and Bauxite Residue

Tao Tian, Chunyue Wu, Liangshen Gong, Chuangye Yao,\* Haifeng Xiao, Lu Liu, and Feng Li



Cite This: *ACS Omega* 2024, 9, 48497–48504



Read Online

ACCESS |



Metrics & More

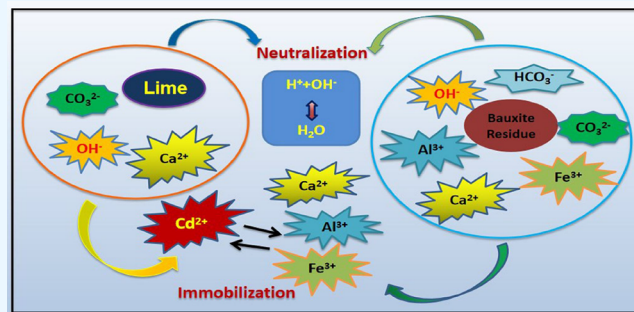


Article Recommendations



Supporting Information

**ABSTRACT:** To immobilize the activity and bioavailability of soil Cd, the single treatment only flooding (F) and the combined treatments with flooding plus bauxite residue (F-B) or lime (F-L) were designed to investigate the impacts of different treatments on the toxicity and bioavailability of Cd in contaminated soil. Compared with the single treatment (F), the combined treatments (F-B and F-L) improved soil-associated organic functional groups and aggregated stability in soil. The average particle sizes of soil aggregates increased from 126 nm (F-treated soil) to 256 and 270 nm following F-B and F-L treatments, respectively. Relative to F treatment, the combined treatments (F-B and F-L) increased soil pH, soil EC, and residual Cd content in soil and reduced exchangeable Cd and acid-soluble Cd content in soil. The exchangeable Cd contents in soils were decreased to 3.17 and 3.42 mg/kg following F-B and F-L treatments in comparison with F-treated soils (4.31 mg/kg), respectively. For the soils with F-B and F-L treatments, soil residual Cd contents increased from 54% (F treatment) to 57 and 56%, respectively, and soil acid-soluble Cd contents decreased from 46% (F treatment) to 37 and 43%, respectively. A negative correlation was found in soil pH versus soil exchangeable Cd and soil acid-soluble Cd. In addition, the F-B treatment exhibited superiority in suppressing toxicity and bioavailability of soil Cd, owing to that F-B treatment is easy to induce neutralization reaction and immobilization effect in contaminated soil. The findings offer evidences that F-B treatment is a facile approach to suppress toxicity and bioavailability of soil Cd, which shows potential for immobilization of Cd in soil.



## 1. INTRODUCTION

The rapid advancement of urbanization and industrialization has led to increased production and mining activities, in which it is easy to discharge toxic metals such as lead, arsenic, and cadmium into the environment. This results in significant soil contamination and poses substantial risks to plants, animals, and humans who come into contact with or consume products from the contaminated areas.<sup>1</sup> Previous research indicated that there are over 10 million contaminated sites in the world, with over 50% being contaminated by toxic metals, which involves in America, Europe, Japan, Korea, and so forth.<sup>2</sup> Recently, the overall situation of soil contamination in China has not been enough satisfied. China has a positive effect on the world's sustainable development by feeding approximately 20% of the world's population with only 9% of the global cultivated land.<sup>3</sup> According to a national survey reported in China (2014), the compositions of inorganic pollutants were mainly caused by toxic metals. The arable-land soils, taking up 19.4%, were faced with toxic metal contamination, which occupied nearly 50 million acres.<sup>4</sup> Therefore, the toxic metal contamination of soil in China occupied large-area soil resources. In particular, the exceedance sites of Cd contamination is as high as 7.0%.<sup>5</sup> Also, Cd has been identified as a carcinogen by the International Agency for Research on Cancer (IARC). It is urgent and

essential to control Cd contamination.<sup>6</sup> It should be noted that Hunan Province in China is known as the hometown of nonferrous metals, where the mining and smelting process caused Cd contamination into the surrounding farmland soil.<sup>7</sup> The mining activities in Hunan Province have resulted in toxic metal contamination up to 28,000 square hectares in soil, accounting for land areas approximately 13.0% in Hunan province. Moreover, Cd content of 58% in the paddy soil exceeded 0.3 mg/kg, achieving the upper threshold of national standards (0.3 mg/kg, GB 15618-2018) in China.<sup>8–11</sup> The cultivated soils adjacent with the mining regions were severely contaminated by toxic metals (e.g., Cd contamination). The regional characteristics of pollutant distribution give a clue for restoration of soil contamination. For example, the typical Cd contamination in Hunan province.<sup>9</sup>

Received: August 3, 2024

Revised: November 8, 2024

Accepted: November 19, 2024

Published: November 25, 2024



To immobilize the activity and bioavailability of soil Cd, many efforts have been implemented, which mainly involves in physical, biological, and chemical approaches.<sup>2,12–14</sup> Among them, the physical method such as surface capping or soil replacement owned the high-cost characteristics and larger labor consumption, being applicable to small contamination sites.<sup>12,15</sup> The biological method could be environmental-friendly for immobilization of soil Cd without secondary pollution, while it is not universal application, limited to a small number of specific plants and functional microorganisms.<sup>16</sup> The chemical method is a unique approach to immobilize soil Cd in the short term via adding substrate or chemical leachates.<sup>2,17</sup> Substrate addition can passivate activities and regulate forms of Cd in contaminated soil. Compared with the substrate application, addition of chemical leachates is easy to bring about secondary pollution, not conducive to long-term immobilization of Cd in contaminated soil.<sup>2,17</sup> Recently, water management has become a technologically important measure in agricultural production, due to their advantages of simple operation and environmental-friendly approach without secondary pollution.<sup>18</sup> Our previous research confirmed that water management such as flooding (F) treatment could effectively immobilize Cd in paddy soils, which is desirable in Cd-contaminated soils.<sup>18</sup> In previous research, alkaline substrate addition is a facile way for immobilizing Cd contamination of acidic soils through acid–base neutralization stabilization, such as alkaline lime.<sup>19,20</sup> Lahori et al. adopted lime to immobilize soil Cd and reported an improvement in lime-amended soils in comparison with the virgin soil.<sup>21</sup> It was worth noting that bauxite residue is a high alkaline solid waste, generated in the process from bauxite ore to alumina production. Bauxite residue is similar to the characteristics of saline-alkali soil, owning high saline-alkali properties, such as pH: 9.2–12.8, electrical conductivity (EC) with 28.4 mS/cm, exchangeable sodium percentage (ESP) with 42–80%, and sodium absorption ratio (SAR) > 30%.<sup>22,23</sup> Moreover, bauxite residue is difficult to dispose due to strong alkalinity and large-scale production.<sup>22</sup> Bauxite residue acts as substrate addition to immobilize soil Cd, which provides an optional way for disposal of large-scale solid waste and enriches the theory of soil formation of bauxite residue.<sup>23</sup> Currently, most of the studies mainly focus on single immobilization method for soil Cd, such as only water management measure or substrate addition.<sup>2,12</sup> There are a few reports on the synergic application of water management and substrate addition.<sup>24</sup> Moreover, a better understanding on the immobilization mechanism of soil Cd is essential due to the Cd-contaminated characteristics of invisibility, accumulativity, and irreversibility in soil.

In this work, it is hypothesized that the combined immobilization method of water management and substrate addition can effectively promote form transformation and immobilization of soil Cd, further suppressing the toxicity and bioavailability of soil Cd. To verify this hypothesis, the combined immobilization effect of water management (long-term flooding, F) and substrate addition (bauxite residue, B, or lime, L) on soil Cd was assessed by soil cultivation experiments using Cd-contaminated soils. Briefly, the main objectives were (i) to test the differences of physicochemical properties of soil Cd and form transformation of soil Cd following different treatments and (ii) to investigate which treatments will exhibit superiority in reducing toxicity and bioavailability of Cd in contaminated soil.

## 2. MATERIALS AND METHODS

**2.1. Materials.** The tested soils were collected from a farmland region near the lead–zinc ore disposal area in Chenzhou, Hunan province, China (26°10' N, 113°62' E). This region belongs to the subtropical monsoon humid climate zone, with average annual values of temperature of about 17.4 °C and precipitation of approximately 1524.2 mm. The soil samples, followed by natural drying, obtained basic properties including pH of 5.45, cation exchange capacity (CEC) of 10.5 cmol/kg, organic matter of 2.0%, and total Cd content of 10.3 mg/kg. Especially, the total Cd content in tested soils exceeds 34 times of the standard value specified by the environmental quality standard for soil (GB15618-2018, China).<sup>10,11</sup> For the substrate materials, bauxite residue is made up of sand (48.1 wt %), silt (51.7 wt %), and clay (0.2 wt %). The main minerals in bauxite residue are hematite, cancrinite, katoite, calcite, diaspore, gibbsite, and tricalcium aluminate. The pH value of bauxite residue is 11.21, and the Cd content of the bauxite residue is 0.02 mg/kg. Lime is mainly composed of CaCO<sub>3</sub>, with a small amount of CaO. The pH value of lime is 8.61, and no content of Cd was examined in lime.

**2.2. Experimental Design.** The research work was carried out by using soil cultivation experiments at Chemistry-Life Building (25°47' N, 113°05' E) of Xiangnan University, located in Chenzhou, Hunan province, China. The soil samples were cultivated in plastic pots with an inner diameter of 300 mm and a height of 240 mm, in which each pot contained 5 kg of soil. The experiments were set with three treatments of (i) long-term flooding mode (F), maintaining 2–3 cm water layer at soil surface, continuous flooding throughout the entire experimental period; (ii) combination mode of flooding and bauxite residue (F-B, 2% bauxite residue); (iii) combination mode of flooding and lime (F-L; 2% lime). Each treatment is repeated three times to obtain the average value, that is, 9 samples in total. To compare with the short-term immobilization effect of different treatments on soil Cd, the experimental period of one month was set, and water addition was conducted every 2 days in this experiment. Collecting the tested samples with an interval of 6 days for examination included pH, Eh, exchangeable Cd, and extraction forms of soil Cd. After the experiment, soil samples were collected and air-dried naturally. Then, the soil samples were sieved through 10-mesh and 100-mesh nylon sieves, and the resultant soil samples were stored for subsequent analysis.

**2.3. Experimental Analysis.** The compositions of soil samples with different treatments were examined by X-ray diffraction instrument (XRD, Rigaku/MiniFlex 600) with Cu K $\alpha$  radiation. The scanning speed was controlled at 5°/min under an accelerating voltage of 40 kV and emission current of 26 mA.<sup>25</sup> The chemical structure of the soil-associated organic functional group was analyzed by using Fourier transformation infrared spectra (FTIR, Thermo-Fisher Nicolet iS20), and collection of spectra was ranged between 500 and 4000 cm<sup>-1</sup>, along with a resolution of 4 cm<sup>-1</sup>.<sup>26</sup> The morphology characteristics and aggregate particles in soil samples were analyzed by a scanning electron microscope (SEM, JSM-6330F), in which the average size of aggregate particle in soil samples was obtained via the Gauss distribution fitting.<sup>26</sup> In addition, the soil pH was examined using a pH meter (PHS-3C, REX, China) with a solid-to-liquid ratio of 1:2.5,<sup>27</sup> and the electrical conductivity (EC) in soil was measured using an electrode method.<sup>28</sup> The cation exchange capacity (CEC) of

soil was measured by using the ammonium acetate method after washing with alcohol,<sup>18</sup> and the organic matter of soil was detected by a potassium dichromate oxidation-weighted method.<sup>27</sup> The total amount of soil Cd involved using a boiling digestion process with aquaregia and perchloric acid as reagents,<sup>27</sup> and a soil sample of 2.00 g was extracted with 20 mL of 0.01 mol/L CaCl<sub>2</sub>. After extraction, the supernatant was filtered through a quantitative filter paper.<sup>18</sup> The European community bureau of reference (BCR) sequential extraction method was used to extract different fractions of Cd present in soil samples,<sup>27</sup> and the extracted forms of Cd in soils involved in acid-soluble state, Fe–Mn oxidation state, organic-bound state, and residual state. The measurement analysis for determining Cd concentrations within digested solutions obtained from soil samples was performed using an inductively coupled plasma optical emission spectrometer (ICP-OES, Optima 8300, PerkinElmer, USA).<sup>27</sup> All sample analysis processes were complied with quality control according to the national standard substance (GBW(E)-070009) of soil, with a Cd recovery rate of 95.8–98.8%. Simultaneously, the blank experiment was set for comparison.

**2.4. Data Analysis.** All experimental results for data fitting and image processing were analyzed by using Office 2010 and Origin 8.5. The SPSS 19.0 software was employed for single-factor analysis to acquire the significant differences of different data. Multiple comparisons were carried out at the significance level of  $P < 0.05$ . The Person correlation analysis method was adopted to the correlation between the soil pH value and the available Cd content in soil.

### 3. RESULTS AND DISCUSSION

As shown in Figure 1, XRD results suggested that the Cd-contaminated soils with different treatments are mainly

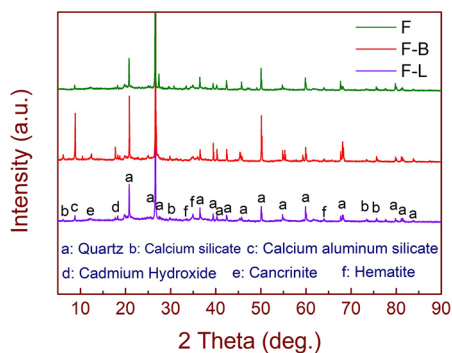


Figure 1. XRD patterns of soil samples following different treatments.

composed of quartz (JCPDS Card No. 46-1045) and other minerals, in which the compounds are in the form of poly crystalline structure.<sup>29</sup> Similar results were reported by Liu et al.<sup>29</sup> Compared with the F-treated soil, the soils following F-B and F-L treatments occurred a weak diffraction peak approximately 6° due to the existence of calcium silicate,<sup>30</sup> which may be ascribed to that bauxite residue and lime introduced Ca<sup>2+</sup> to silicon compounds, promoting the formation of calcium silicate.<sup>31</sup> Calcium silicate in XRD characterization is in accordance with Ca<sub>2</sub>SiO<sub>4</sub> (JCPDS Card No. 24-0034), belonging to the orthorhombic structure.<sup>30</sup> Furthermore, XRD characterization of the soils with F-B treatment indicated the presence of a significant diffraction peak nearly 10° with high relative-diffraction intensity,

corresponding to calcium aluminum silicate,<sup>32</sup> which is attributed to that bauxite residue owns higher concentration of aluminum element.<sup>33</sup> Calcium aluminum silicate in XRD patterns is in coincidence with Ca<sub>3</sub>Al<sub>6</sub>Si<sub>2</sub>O<sub>16</sub> (JCPDS Card No. 23-0105), belonging to the hexagonal structure.<sup>32</sup> In addition, the diffraction peaks located in the 15–20° ranges were matched with JCPDS Card No. 40-0760, in accordance with cadmium hydroxide. The weak peaks with low relative-diffraction intensity of cadmium hydroxide suggested lower contents as compared with other minerals in soil. The diffraction peaks corresponding to cancrinite and hematite could be matched with JCPDS Card No. 48-0733 and JCPDS Card No. 52-1449, respectively.<sup>23</sup>

Figure 2 displays the FTIR spectra of Cd-contaminated soils with different treatments. It can be seen that the four

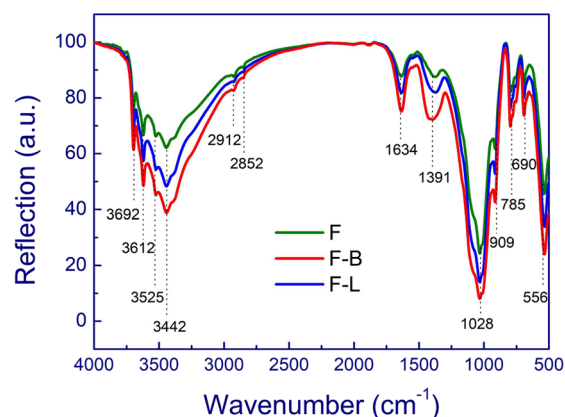


Figure 2. FTIR spectra of soil samples following different treatments.

distinctive peaks (3692, 3612, 3525, and 3442 cm<sup>-1</sup>) at higher wavenumber ranges can be assigned to the –OH stretching vibration mode of hydroxyl groups,<sup>26,34,35</sup> and the two weak-signal peaks (2912 and 2852 cm<sup>-1</sup>) are in accordance with C–H stretching bands.<sup>36</sup> The absorption bands located at 1634, 1391, and 1028 cm<sup>-1</sup> can be ascribed to the C–C/C–O stretching vibration mode, C–H stretching vibration mode, and C–O stretching vibration mode, respectively.<sup>26</sup> The peak with 909 cm<sup>-1</sup> maybe attributed to the Al–Al–OH or Al–OH–Al stretching vibration mode from aluminum-based minerals.<sup>37,38</sup> The three peaks at lower wavenumber ranges with 785, 690, and 556 cm<sup>-1</sup> can be assigned to the Si–O, Si–O–Si, and O–Si–O stretching vibration modes from quartz in soil, respectively.<sup>37,38</sup> The intensity of the absorption bands in Figure 2 reflected soil-associated organic functional group characteristics (i.e., amounts and quantities), and the results indicated reasonable differences for soils following different treatments in spite of similarity in FTIR spectra shape for all treatments, especially significant intensity in F-B mode, which revealed that amounts of organic functional groups in soil are affected by the substrate application.

Figure 3 shows the morphology characteristics of soil aggregates through SEM observation, in which the aggregate structure occurred evolution following different treatments. As can be seen, F-treated soils presented that small aggregates exhibited dispersedly distribution. According to the SEM characterization, the sizes of aggregate particles were obtained, and the average particle size of soil aggregates with F treatment was approximately ~126 nm (Supporting Information Figure S1). However, bigger soil aggregates could be formed following

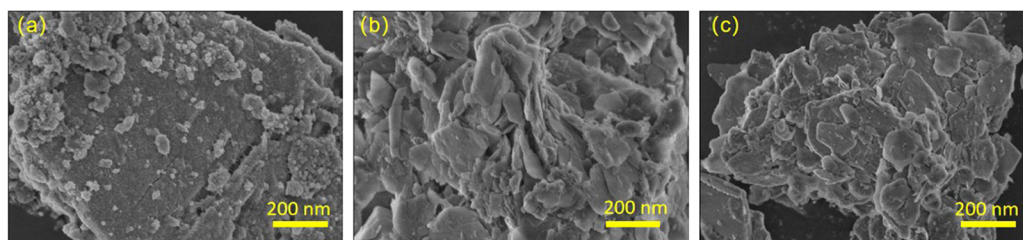


Figure 3. Morphology characteristics of soil samples following different treatments: (a) F, (b) F-B, and (c) F-L treatments.

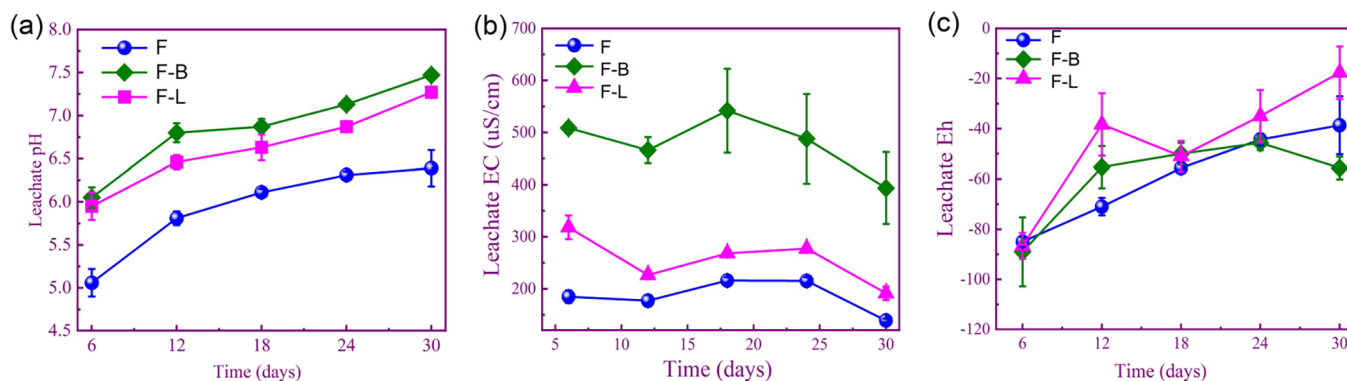


Figure 4. Variations of (a) pH, (b) EC, and (c) Eh of soil leachates following different treatments.

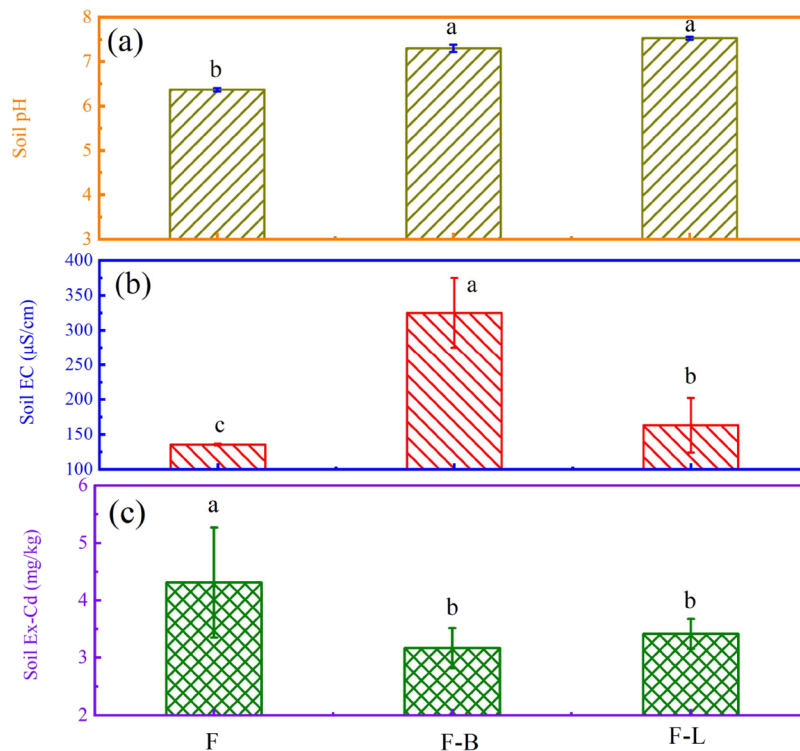


Figure 5. Variations of (a) soil pH, (b) soil EC, and (c) soil exchangeable Cd contents following different treatments.

F-B and F-L treatments in Figure 3. The corresponding average sizes of aggregates following F-B and F-L treatments were about to be  $\sim 256$  and  $\sim 270$  nm, respectively (Supporting Information Figure S1). SEM characterization results suggested that F-B and F-L treatments can enhance aggregate size, further improving aggregate stability and soil quality.<sup>39</sup> In general, toxic metals (e.g., Cd) in soil preferred to accumulate in fine soil aggregate, and accumulation factors for soil Cd

assessment in microaggregates were high.<sup>40</sup> Therefore, the enhancement of aggregate sizes easily forms macroaggregates, further changing the distribution and accumulation of Cd in soil aggregates.

As shown in Figure 4, the impacts of different treatments on the physicochemical properties of soil leachate were investigated. Figure 4a illustrates that the pH of soil leachate increased as the flooding time increased for all treatments,

exhibiting time-dependent characteristics irrespective of different treatments. This result maybe because of gradual consumption of  $H^+$  during the continuous flooding process, and the flooding mode increases the pH value.<sup>41</sup> Compared with F-treated leachate pH, the values of leachate pH following F-B and F-L treatments can be significantly enhanced, which is due to that bauxite residue of F-B treatment and lime of F-L treatment are high alkaline characteristics, further mediating pH of soil leachate in terms of neutralization reaction.<sup>22,42</sup> Particularly, for the F-B treatment, the pH variation of soil leachate is most significant, owing to that bauxite residue of F-B treatment has extreme alkalinity.<sup>22</sup> In Figure 4b, the leachate EC values exhibited an obvious fluctuation with increasing leachate time, while the values of leachate EC at the same time can follow the order of F-B > F-L > F. This result can be attributed to that the addition of bauxite residue or lime can introduce cations into soil solution, and more cation types were introduced following F-B treatment relative to F-L treatment.<sup>22,43,44</sup> As depicted in Figure 4c, irrespective of different treatments, Eh value of soil leachate increased with increasing leachate time, and insignificant differences following different treatments were found due to that soil leachate always maintained reduction potential after the flooding state.<sup>18</sup>

The physicochemical properties of soils following different treatments were also studied, as shown in Figure 5. Figure 5a presents the variations of soil pH following different treatments, where F-B and F-L treatments increased soil pH due to the alkaline characteristics of bauxite residue and lime.<sup>22,42</sup> Usually, the increase of soil pH can decrease the concentration of soil Cd.<sup>45,46</sup> Sun et al. investigated the sepiolite material for Cd-polluted soil restoration and reported that the addition of sepiolite material increased soil pH and decreased the toxicity characteristic leaching procedure-Cd (TCLP-Cd) concentration.<sup>45</sup> Also, Novak et al. adopted the substrate addition method with biochar and lime amendments to dispose mine spoil soil and reported that substrate application can increase soil pH, further reducing the extractable metal concentrations in soil.<sup>46</sup> Furthermore, soil EC values with different treatments were investigated and are shown in Figure 5b. It is evident that F-B treated soils achieved an obvious increase of EC value compared with other treatments because of that bauxite residue of F-B treatment contains more cation types.<sup>22,43,44</sup> In addition, the exchangeable Cd content in contaminated soil is related to activity and mobility of soil Cd, which can endanger plant growth and human health.<sup>18</sup> As displayed in Figure 5c, compared with F treatment (4.31 mg/kg), soil exchangeable Cd contents were decreased to 3.17 and 3.42 mg/kg following F-B and F-L treatments, respectively. Among them, the F-B treatment exhibited superiority for the reduction of exchangeable Cd in contaminated soil, which provides potential for immobilizing Cd in contaminated soil.

To better understand the form transformation of soil Cd following different treatments, the distribution of soil Cd with various fractions was studied, as depicted in Figure 6. It is clear that soil Cd is mainly in the form of residual Cd (O-Cd) and acid-soluble Cd (AC-Cd), and a small quantity of organic-bound Cd (Org-Cd) and Fe/Mn-bound Cd (Fe/Mn-Cd) was found. Compared with soil residual Cd content in the F treatment (54%), the proportions of soil residual Cd contents increased to 57 and 56% following F-B and F-L treatments, respectively, which indicated that F-B treatment can more effectively immobilize soil Cd bioavailability.<sup>29</sup> In contrast, as compared to soil acid-soluble Cd content in the F-treatment

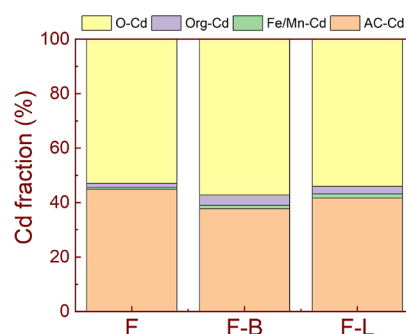


**Figure 6.** Effects of different treatments on the distribution of Cd fractions in soil (O-Cd: residual Cd, Org-Cd: organic-bound Cd, Fe/Mn-Cd: Fe/Mn-bound Cd, and AC-Cd: acid-soluble Cd).

(46%), the proportions of soil acid-soluble Cd contents decreased to 37 and 43% following F-B and F-L treatments, respectively, which further confirmed that the combined treatments (F-B and F-L) can suppress the bioavailability of soil Cd, and the F-B treatment achieved a better immobilization effect of Cd in contaminated soil.

Correlation analysis from Figure 7 indicated that a negative correlation was observed between soil pH and soil exchange-

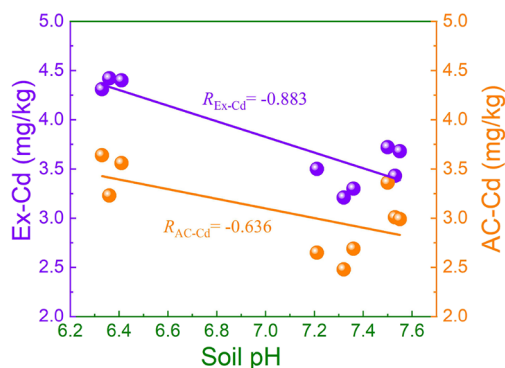


**Figure 7.** Correlations analysis of soil pH versus exchangeable Cd contents and acid-soluble Cd contents in soil.

able Cd ( $R = -0.883$ ,  $P < 0.05$ ), and the relationship between soil pH and soil acid-soluble Cd also exhibited a negative correlation ( $R = -0.636$ ,  $P < 0.05$ ). Therefore, it can be concluded that variation of pH is easy to change soil exchangeable Cd content and soil acid-soluble Cd content, and pH regulation is beneficial for immobilization of Cd in soil. Substrate applications such as bauxite residue and lime can increase soil pH in suitable ranges during the flooding state (Figure 5), which provides a feasible approach to immobilize soil Cd.

Based on the aforementioned analysis and discussion, we proposed the interference mechanism of Cd-contaminated soils following F-B and F-L treatments, as shown in Figure 8. On the one hand, the neutralization reaction can be occurred in Cd-contaminated soils following F-B and F-L treatments, because bauxite residue/lime is easy to release  $OH^-$  due to their alkaline characteristics and the untreated soil tends to be acidic (containing  $H^+$ ).<sup>22,42</sup> Therefore, the F-B and F-L treatments can increase soil pH (Figure 5) and decrease soil exchangeable Cd content and soil acid-soluble Cd content (Figure 7), further immobilizing Cd and suppressing the toxicity and bioavailability of Cd in soil. On the other hand, the

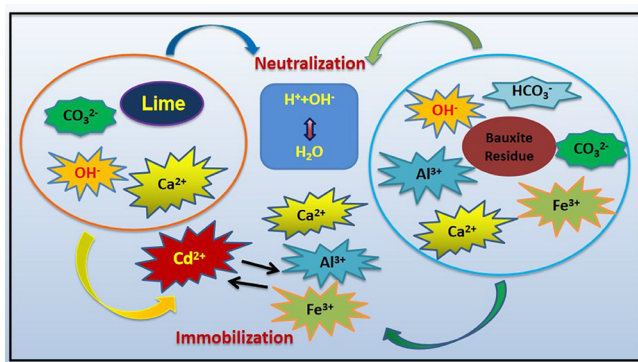


**Figure 8.** Schematic representation showing the interference mechanisms of Cd-contaminated soils following F-B and F-L treatments.

concentrations of cations can be modulated by bauxite residue of F-B treatment and lime of F-L treatment, which promotes the immobilization of soil Cd.<sup>20,47</sup> For the F-L treated soils, more  $\text{Ca}^{2+}$  could be generated in soil owing to lime addition, and the Cd contaminant was embedded in the interstices of the soil calcium interfaces, making them inert and immobile.<sup>20</sup> For the F-B treated soils, Cd ions were immobilized by means of ion exchange effect, in which the cadmium ions in soil could be adsorbed and trapped by bauxite residue via the cation exchange process.<sup>47</sup> In this experiment, bauxite residue of F-B treatment is a high-alkalinity substance,<sup>22</sup> which can increase pH under the flooding mode by means of neutralization reaction. The increase of soil pH can reduce the exchangeable Cd content in contaminated soil.<sup>48</sup> In addition, incorporating bauxite residue of F-B treatment can induce the release of more cations (i.e.,  $\text{Al}^{3+}$ ,  $\text{Ca}^{2+}$ , and  $\text{Fe}^{3+}$ ),<sup>22</sup> and these cations into soil can promote the immobilization of soil Cd in terms of cation exchange effect.<sup>21,46–48</sup> Moreover, bauxite residue owns more cation types and higher EC value (Figure 5), which results in that more cadmium ions in soil were immobilized. Therefore, the neutralization and immobilization effects of Cd in F-B-treated soils are more forceful relative to F-L treatment, which caused that F-B treatment exhibits superiority in suppressing toxicity and bioavailability of soil Cd.

#### 4. CONCLUSIONS

The results obtained in the present study demonstrated that F-B and F-L treatments can regulate the amounts of organic functional groups and the aggregate stability in Cd-contaminated soil. Both F-B and F-L treatments were considerably effective in regulating leachate pH, leachate EC, soil pH, soil EC, exchangeable Cd content, and acid-soluble Cd content in soil. The relationship of negative correlation was found in soil pH versus exchangeable Cd content and acid-soluble Cd content in soil. It is worthy to mention that F-B treatment performed superiority in suppressing toxicity and bioavailability of soil Cd, which can be attributed to that F-B treatment easily induces neutralization reaction and immobilization effect in Cd-contaminated soils. These findings provide valuable insight into the immobilization of soil Cd and the suppression of the toxicity and bioavailability of Cd in contaminated soil.

#### ■ ASSOCIATED CONTENT

##### SI Supporting Information

The Supporting Information is available free of charge at <https://pubs.acs.org/doi/10.1021/acsomega.4c07130>.

Size distribution of soil aggregate particles (PDF)

#### ■ AUTHOR INFORMATION

##### Corresponding Author

**Chuangye Yao** – Microelectronics and Optoelectronics Technology Key Laboratory of Hunan Higher Education, School of Physics and Electronic Electrical Engineering, Xiangnan University, Chenzhou 423000, China; [orcid.org/0009-0002-8456-9378](https://orcid.org/0009-0002-8456-9378); Email: [yaochuangye@xnu.edu.cn](mailto:yaochuangye@xnu.edu.cn)

##### Authors

**Tao Tian** – Hunan Provincial Key Laboratory of Xiangnan Rare-Precious Metals Compounds and Application, School of Chemistry and Environmental Science, Xiangnan University, Chenzhou 423000, China

**Chunyu Wu** – Hunan Provincial Key Laboratory of Xiangnan Rare-Precious Metals Compounds and Application, School of Chemistry and Environmental Science, Xiangnan University, Chenzhou 423000, China

**Liangshen Gong** – Hunan Provincial Key Laboratory of Xiangnan Rare-Precious Metals Compounds and Application, School of Chemistry and Environmental Science, Xiangnan University, Chenzhou 423000, China

**Haifeng Xiao** – Hunan Provincial Key Laboratory of Xiangnan Rare-Precious Metals Compounds and Application, School of Chemistry and Environmental Science, Xiangnan University, Chenzhou 423000, China

**Lu Liu** – Hunan Provincial Key Laboratory of Xiangnan Rare-Precious Metals Compounds and Application, School of Chemistry and Environmental Science, Xiangnan University, Chenzhou 423000, China

**Feng Li** – Hunan Provincial Key Laboratory of Xiangnan Rare-Precious Metals Compounds and Application, School of Chemistry and Environmental Science, Xiangnan University, Chenzhou 423000, China

Complete contact information is available at: <https://pubs.acs.org/10.1021/acsomega.4c07130>

##### Notes

The authors declare no competing financial interest.

#### ■ ACKNOWLEDGMENTS

This study was supported by the Hunan Provincial Natural Science Foundation of China (Grant Nos. 2022JJ40414 and 2024JJ7512), the Scientific Research Fund of Hunan Provincial Education Department (Grant No. 23B0782), the Research Foundation of the Department of Natural Resources of Hunan Province, China (Grant No. 20230140ST), the Applied Characteristic Discipline of Electronic Science and Technology of Xiangnan University (Grant No. XNXY20221210), the Scientific Research Program of Xiangnan University (Grant Nos. 2021XJ36, 2023XJ05, and 2024XJ70), and the College students' Innovation and Entrepreneurship Training Program of Xiangnan University (Grant Nos. X2023050 and X2023054).

## REFERENCES

- (1) Sahito, Z. A.; Zehra, A.; Yu, S.; Chen, S.; He, Z.; Yang, X. Chinese Sapindaceous Tree Species (*Sapindus Mukorosii*) Exhibits Lead Tolerance and Long-Term Phytoremediation Potential for Moderately Contaminated Soils. *Chemosphere* **2023**, *338*, No. 139376.
- (2) Xu, D.; Fu, R.; Wang, J.; Shi, Y.; Guo, X. Chemical Stabilization Remediation for Heavy Metals in Contaminated Soils on the Latest Decade: Available Stabilizing Materials and Associated Evaluation Methods- A Critical Review. *J. Clean. Prod.* **2021**, *321*, No. 128730.
- (3) Ren, S.; Song, C.; Ye, S.; Cheng, C.; Gao, P. The Spatiotemporal Variation in Heavy Metals in China's Farmland Soil over the Past 20 Years: A Meta-Analysis. *Sci. Total Environ.* **2022**, *806*, No. 150322.
- (4) Jin, Y.; Gao, T.; Zhao, B.; Liu, Y.; Liu, C.; Qin, M. Modeling Spatial Trends and Exchange Fluxes of Contaminants in Agricultural Soil under Pollution Prevention Measures. *J. Environ. Manage.* **2024**, *354*, No. 120419.
- (5) Yang, J.; Hu, R.; Zhao, C.; Wang, L.; Lei, M.; Guo, G.; Shi, H.; Liao, X.; Chen, T. Challenges and Opportunities for Improving the Environment Quality of Cadmium-Contaminated Soil in China. *J. Hazard. Mater.* **2023**, *445*, No. 130560.
- (6) Wu, Y.; He, H.; Ren, J.; Shen, H.; Sahito, Z. A.; Li, B.; Tang, X.; Tao, Q.; Huang, R.; Wang, C. Assembly Patterns and Key Taxa of Bacterial Communities in the Rhizosphere Soil of Moso Bamboo (*Phyllostachys Pubescens*) under Different Cd and Pb Pollution. *Int. J. Phytoremediat.* **2024**, *26*, 1776–1786.
- (7) Zhao, J.; Luo, Q.; Ding, L.; Fu, R.; Zhang, F.; Cui, C. Valency Distributions and Geochemical Fractions of Arsenic and Antimony in Non-Ferrous Smelting Soils with Varying Particle Sizes. *Ecotox. Environ. Safe.* **2022**, *233*, No. 113312.
- (8) Li, X.; Zhao, Z.; Yuan, Y.; Wang, X.; Li, X. Heavy Metal Accumulation and Its Spatial Distribution in Agricultural Soils: Evidence from Hunan Province, China. *RSC Adv.* **2018**, *8*, 10665–10672.
- (9) Wang, W.; Chen, W.; Peng, C. Risk Assessment of Cd Polluted Paddy Soils in the Industrial and Township Areas in Hunan, Southern China. *Chemosphere* **2016**, *144*, 346–351.
- (10) Shi, T.; Zhang, Y.; Gong, Y.; Ma, J.; Wei, H.; Wu, X.; Zhao, L.; Hou, H. Status of Cadmium Accumulation in Agricultural Soils across China (1975–2016): From Temporal and Spatial Variations to Risk Assessment. *Chemosphere* **2019**, *230*, 136–143.
- (11) Jiang, Z.; Guo, Z.; Peng, C.; Liu, X.; Zhou, Z.; Xiao, X. Heavy Metals in Soils around Non-Ferrous Smelters in China: Status, Health Risks and Control Measures. *Environ. Pollut.* **2021**, *282*, No. 117038.
- (12) Song, P.; Xu, D.; Yue, J.; Ma, Y.; Dong, S.; Feng, J. Recent Advances in Soil Remediation Technology for Heavy Metal Contaminated Sites: A Critical Review. *Sci. Total Environ.* **2022**, *838*, No. 156417.
- (13) Hsu, C.; Cheng, Y.; Chung, A.; Huang, Y.; Ting, Y.; Hsi, H. Using Recoverable Sulfurized Magnetic Biochar for Active Capping to Remediate Multiple Heavy Metal Contaminated Sediment. *Environ. Pollut.* **2023**, *316*, No. 120555.
- (14) Meng, H.; Hu, S.; Hong, Z.; Chi, W.; Chen, G.; Cheng, K.; Wang, Q.; Liu, T.; Li, F.; Liu, K.; Yang, Y. Effects of Zero-Valent Iron Added in the Flooding or Drainage Process on Cadmium Immobilization in an Acid Paddy Soil. *J. Environ. Sci.* **2024**, *138*, 19–31.
- (15) Liu, L.; Li, W.; Song, W.; Guo, M. Remediation Techniques for Heavy Metal-Contaminated Soils: Principles and Applicability. *Sci. Total Environ.* **2018**, *633*, 206–219.
- (16) Mo, T.; Jiang, D.; Shi, D.; Xu, S.; Huang, X.; Huang, Z. Remediation Mechanism of “Double-Resistant” Bacteria-*Sedum Alfredii Hance* on Pb- and Cd-Contaminated Soil. *Ecol. Process.* **2022**, *11*, 20.
- (17) Arwidsson, Z.; Elgh-Dalgren, K.; von Kronhelm, T.; Sjöberg, R.; Allard, B.; van Hees, P. Remediation of Heavy Metal Contaminated Soil Washing Residues with Amino Polycarboxylic Acids. *J. Hazard. Mater.* **2010**, *173*, 697–704.
- (18) Tian, T.; Zhou, H.; Gu, J.; Jia, R.; Li, H.; Wang, Q.; Zeng, M.; Liao, B. Cadmium Accumulation and Bioavailability in Paddy Soil under Different Water Regimes for Different Growth Stages of Rice (*Oryza Sativa L.*). *Plant Soil* **2019**, *440*, 327–339.
- (19) Li, W.; Ni, P.; Yi, Y. Comparison of Reactive Magnesia, Quick Lime, and Ordinary Portland Cement for Stabilization/Solidification of Heavy Metal-Contaminated Soils. *Sci. Total Environ.* **2019**, *671*, 741–753.
- (20) Moghal, A. A. B.; Mohammed, S. A. S.; Almajed, A.; Al-Shamrani, M. A. Desorption of Heavy Metals from Lime-Stabilized Arid-Soils using Different Extractants. *Int. J. Civ. Eng.* **2020**, *18*, 449–461.
- (21) Hussain Lahori, A.; Zhang, Z.; Guo, Z.; Mahar, A.; Li, R.; Kumar Awasthi, M.; Ali Sial, T.; Kumbhar, F.; Wang, P.; Shen, F.; Zhao, J.; Huang, H. Potential Use of Lime Combined with Additives on (Im)mobilization and Phytoavailability of Heavy Metals from Pb/Zn Smelter Contaminated Soils. *Ecotox. Environ. Safe.* **2017**, *145*, 313–323.
- (22) Tian, T.; Zhang, C.; Zhu, F.; Yuan, S.; Guo, Y.; Xue, S. Effect of Phosphogypsum on Saline-Alkalinity and Aggregate Stability of Bauxite Residue. *Trans. Nonferrous Met. Soc. China* **2021**, *31*, 1484–1495.
- (23) Tian, T.; Ke, W.; Zhu, F.; Wang, Q.; Ye, Y.; Guo, Y.; Xue, S. Effect of Substrate Amendment on Alkaline Minerals and Aggregate Stability in Bauxite Residue. *J. Cent. South Univ.* **2019**, *26*, 393–403.
- (24) Weijie, X.; Shuzhen, H.; AmanKhan, M.; Yu, C.; Linlin, X.; Zebin, R.; Liu, H.; Zhenhua, C.; Shengwei, C.; Ye, Z.; Liu, D. Effect of Water and Fertilization Management on Cd Immobilization and Bioavailability in Cd-Polluted Paddy Soil. *Chemosphere* **2021**, *276*, No. 130168.
- (25) Yao, C.; Hao, A.; Thatikonda, S. K.; Huang, W.; Qin, N.; Bao, D. Realization of Resistive and Magnetization Switching in Sol-Gel Derived Yttrium Iron Garnet Thin Films. *Thin Solid Films* **2020**, *699*, No. 137889.
- (26) Tian, T.; Liu, Z.; Zhu, F.; Hartley, W.; Ye, Y.; Xue, S. Improvement of Aggregate-Associated Organic Carbon and Its Stability in Bauxite Residue by Substrate Amendment Addition. *Land Degrad. Dev.* **2020**, *31*, 2405–2416.
- (27) Zhou, H.; Wang, Z.; Li, C.; Yuan, H.; Hu, L.; Zeng, P.; Yang, W.; Liao, B.; Gu, J. Straw Removal Reduces Cd Availability and Rice Cd Accumulation in Cd-Contaminated Paddy Soil: Cd Fraction, Soil Microorganism Structure and Porewater DOC and Cd. *J. Hazard. Mater.* **2024**, *476*, No. 135189.
- (28) Tian, T.; Zhou, J.; Zhu, F.; Ye, Y.; Guo, Y.; Hartley, W.; Xue, S. Effect of Amendments on the Leaching Behavior of Alkaline Anions and Metal Ions in Bauxite Residue. *J. Environ. Sci.* **2019**, *85*, 74–81.
- (29) Liu, Y.; Zhang, C.; Wu, K.; Liu, S. Sustainable Stabilization/Solidification of Cd and Pb in Industrially Heavy Metal-Contaminated Site Soils using A Novel Binder Incorporating Bone Meal and Fly Ash. *Constr. Build. Mater.* **2024**, *416*, No. 135162.
- (30) Wong, K.; Li, Y.; Yang, H.; Chien, C.; Kao, L.; Lin, T.; Yang, T.; Shih, C. Antimicrobial Properties of Bimetallic-Containing Mesoporous Bioglass Against *Enterococcus Faecalis*. *J. Dent. Sci.* **2024**, In Press.
- (31) Liao, C.; Zeng, L.; Shih, K. Quantitative X-ray Diffraction (QXRD) Analysis for Revealing Thermal Transformations of Red Mud. *Chemosphere* **2015**, *131*, 171–177.
- (32) Huang, Y.; Wang, M.; Li, Z.; Gong, Y.; Zeng, E. Y. *In Situ* Remediation of Mercury-Contaminated Soil using Thiol-Functionalized Graphene Oxide/Fe-Mn Composite. *J. Hazard. Mater.* **2019**, *373*, 783–790.
- (33) Huang, X.; Zhang, Q.; Wang, W.; Pan, J.; Yang, Y. Effect of Carbide Slag on Removal of Na<sup>+</sup>/K<sup>+</sup> from Red Mud Based on Water Leaching. *ACS Omega* **2022**, *7*, 4101–4109.
- (34) Jing, Y.; Chen, R.; Zhang, J.; Hu, L.; Qiu, X. Developed Recyclable CaFe-Layered Double Hydroxide for Efficient Cadmium Immobilization in Soil: Performance and Bioavailability. *Miner.* **2024**, *14*, 656.

- (35) Tan, J.; Li, Z.; Zhao, G.; Guo, G.; Zhang, H.; Wang, S. Modified Bentonite As a Dissolve-Extrusion Composite and Its Modification Mechanism. *ACS Omega* **2024**, *9*, 33900–33911.
- (36) Chouchene, K.; Nacci, T.; Modugno, F.; Castelvetro, V.; Ksibi, M. Soil Contamination by Microplastics in Relation to Local Agricultural Development as Revealed by FTIR, ICP-MS and Pyrolysis-GC/MS. *Environ. Pollut.* **2022**, *303*, No. 119016.
- (37) Ene, A.; Moraru, S. S.; Moraru, D. I.; Pantelica, A.; Gosav, S.; Ceoromila, A. M. Mahor and Trace Element Accumulation in Soils and Crops (Wheat, Corn, Sunflower) around Steel Industry in the Lower Danube Basin and Associated Ecological and Health Risks. *Appl. Sci.* **2024**, *14*, 5616.
- (38) Krivoshein, P. K.; Volkov, D. S.; Rogova, O. B.; Proskurnin, M. A. FTIR Photoacoustic and ATR Spectroscopies of Soils with Aggregate Size Fractionation by Dry Sieving. *ACS Omega* **2022**, *7*, 2177–2197.
- (39) Sun, Q.; Meng, J.; Lan, Y.; Shi, G.; Yang, X.; Cao, D.; Chen, W.; Han, X. Long-Term Effects of Biochar Amendment on Soil Aggregate Stability and Biological Binding Agents in Brown Earth. *Catena* **2021**, *205*, No. 105460.
- (40) Shen, Q.; Wu, M.; Zhang, M. Accumulation and Relationship of Metals in Different Soil Aggregate Fractions Along Soil Profiles. *J. Environ. Sci.* **2022**, *115*, 47–54.
- (41) Li, J.; Xu, Y. Immobilization Remediation of Cd-Polluted Soil with Different Water Condition. *J. Environ. Manag.* **2017**, *193*, 607–612.
- (42) Nazar, S.; Yang, J.; Ashraf, M.; Aslam, F.; Javed, M. F.; Eldin, S. M.; Xie, J. Formulation and Characterization of Cleaner One-Part Novel Fly Ash/Lime-Based Alkali-Activated Material. *J. Mater. Res. Technol.* **2023**, *23*, 3821–3839.
- (43) Corwin, D. L.; Scudiero, E. Field-Scale Apparent Soil Electrical Conductivity. *Soil Sci. Soc. Am. J.* **2020**, *84*, 1405–1441.
- (44) Paz, A. M.; Castanheira, N.; Farzaman, M.; Paz, M. C.; Gonçalves, M. C.; Monteiro Santos, F. A.; Triantafyllis, J. Prediction of Soil Salinity and Sodicity using Electromagnetic Conductivity Imaging. *Geoderma*. **2020**, *361*, No. 114086.
- (45) Sun, Y.; Sun, G.; Xu, Y.; Wang, L.; Lin, D.; Liang, X.; Shi, X. In Situ Stabilization Remediation of Cadmium Contaminated Soils of Wastewater Irrigation Region Using Sepiolite. *J. Environ. Sci.* **2012**, *24*, 1799–1805.
- (46) Novak, J. M.; Ippolito, J. A.; Ducey, T. F.; Watts, D. W.; Spokas, K. A.; Trippe, K. M.; Sigua, G. C.; Johnson, M. G. Remediation of An Acidic Mine Spoil: Miscanthus Biochar and Lime Amendment Affects Metal Availability, Plant Growth, and Soil Enzyme Activity. *Chemosphere* **2018**, *205*, 709–718.
- (47) Yang, D.; Wang, R.; Feng, X.; Chu, Z.; Li, J.; Wei, W.; Zheng, R.; Zhang, J.; Chen, H. Transferring Waste Red Mud into Ferric Oxide Decorated ANA-Type Zeolite for Multiple Heavy Metals Polluted Soil Remediation. *J. Hazard. Mater.* **2022**, *424*, No. 127244.
- (48) Mai, X.; Tang, J.; Tang, J.; Zhu, X.; Yang, Z.; Liu, X.; Zhuang, X.; Feng, G.; Tang, L. Research Progress on the Environmental Risk Assessment and Remediation Technologies of Heavy Metal Pollution in Agricultural Soil. *J. Environ. Sci.* **2025**, *149*, 1–20.